How Neutral is the Intergalactic Medium at $z \sim 6$?

Adam Lidz[a], Lam Hui[a], Matias Zaldarriaga[b,c] and Roman Scoccimarro[b]

[a] Department of Physics, Columbia University, 538 West 120th Street, New York, NY 10027
[b] Physics Department, New York University, 4 Washington Place, New York, NY 10003
[c] Institute for Advanced Study, Einstein Drive, Princeton NJ 08540
lidz@astro.columbia.edu, lhui@astro.columbia.edu, matiasz@physics.nyu.edu, scoccima@physics.nyu.edu

ABSTRACT

Recent observations of high redshift quasar spectra reveal long gaps with little flux. A small or no detectable flux does not by itself imply the intergalactic medium (IGM) is neutral. Inferring the average neutral fraction from the observed absorption requires assumptions about clustering of the IGM, which the gravitational instability model supplies. Our most stringent constraint on the neutral fraction at $z \sim 6$ is derived from the mean Lyman-beta transmission measured from the $z = 6.28$ SDSS quasar of Becker et al. – the neutral hydrogen fraction at mean density has to be larger than 4.7×10^{-4}. This is substantially higher than the neutral fraction of $\sim 3 - 5 \times 10^{-5}$ at $z = 4.5 - 5.7$, suggesting that dramatic changes take place around or just before $z \sim 6$, even though current constraints are still consistent with a fairly ionized IGM at $z \sim 6$. These constraints translate also into constraints on the ionizing background, subject to uncertainties in the IGM temperature. An interesting alternative method to constrain the neutral fraction is to consider the probability of having many consecutive pixels with little flux, which is small unless the neutral fraction is high. It turns out that this constraint is slightly weaker than the one obtained from the mean transmission. We show that while the derived neutral fraction at a given redshift is sensitive to the power spectrum normalization, the size of the jump around $z \sim 6$ is not. We caution that the main systematic uncertainties include spatial fluctuations in the ionizing background, and the continuum placement. Tests are proposed. In particular, the sightline to sightline dispersion in mean transmission might provide a useful diagnostic. We express the dispersion in terms of the transmission power spectrum, and develop a method to calculate the dispersion for spectra that are longer than the typical simulation box.

Subject headings: cosmology: theory – intergalactic medium – large scale structure of universe; quasars – absorption lines

1. Introduction

Recent spectroscopic observations of $z \gtrsim 4.5$ quasars discovered by the Sloan Digital Sky Survey (SDSS) have opened up new windows into the study of the high redshift intergalactic medium (IGM) (Fan et al. 2000, Zheng et al. 2000, Schneider et al. 2001, Anderson et al. 2001 Fan et al. 2001a, Becker et al. 2001, Djorgovski et al. 2001). In particular, Becker et al. (2001) observed Gunn-Peterson troughs (Gunn & Peterson 1965) in the spectrum of a $z = 6.28$ quasar, which were interpreted as suggesting that the universe was close to the reionization epoch at $z \sim 6$.

That the absorption increases quickly with redshift is not by itself surprising: ionization equilibrium tells us that the neutral hydrogen density is proportional to the gas density squared, which is proportional to $(1+z)^6$ at the cosmic mean. The evolution of the ionizing background and gas temperature will modify this redshift dependence, but the rapid evolution of absorption remains a robust outcome. What is interesting, as Becker et al. (2001) emphasized, is that the observed mean transmission at redshift $z \sim 6$ is lower than what one would expect based on an extrapolation of the column density distribution and its redshift evolution (number density of clouds scaling as $\sim (1+z)^{2.5}$) from lower redshifts. On the other hand, the popular gravitational instability theory of structure formation provides detailed predictions for how the IGM should be clustered, and how this clustering evolves with redshift, which has been shown to be quite successful when compared with observations at $z \sim 2-4$ (See e.g. Cen et al. 1994, Zhang et al. 1995, Reisenegger & Miralda-Escudé 1995, Hernquist et al. 1996, Miralda-Escudé 1996, Muecket et al. 1996, Bi & Davidsen 1997, Bond & Wadsley 1997, Hui et al. 1997, Croft et al. 1998, Theuns et al. 1999, Bryan et al. 1999, McDonald et al. 2000a). These predictions allow us to directly infer the neutral fraction of the IGM from the observed absorption (the relation between the two depends on the nature of clustering of the IGM), and so can further inform our interpretations of the recent $z \sim 6$ results.

How neutral is the IGM at $z \sim 6$, and how different is the neutral fraction compared to lower redshifts? These are the questions we would like to address quantitatively, making use of the gravitational instability model of the IGM.

The paper is organized as follows. First, we start with a brief description of the gravitational instability model for the IGM and the simulation technique in §2. In §3.1, we derive the neutral hydrogen fraction $X_{\rm HI}$, and equivalently the level of ionizing flux $J_{\rm HI}$, at several different redshifts leading up to $z \sim 6$ from the observed mean Lyman-alpha (Lyα) transmission. This exercise using the Lyα spectrum is similar to the one carried out in McDonald & Miralda-Escudé (2001), except for the addition of new high redshift data. [1] We then examine in §3.2 the constraints on the same quantities $X_{\rm HI}$ and $J_{\rm HI}$ from the observed mean Lyman-beta (Lyβ) transmission, Lyβ being particularly useful at high Lyα optical depth, because the Lyβ absorption cross-section is a factor of ~ 5 smaller than the Lyα cross-section. The goal here is to use Lyβ absorption to obtain constraints on $X_{\rm HI}$ and $J_{\rm HI}$ that are as stringent as possible. In §3.2, we also examine the sensitivity of our conclusions to the power spectrum normalization.

An intriguing question is: instead of focusing on the mean transmission, can one make use of the fact that the observed spectrum at $z \sim 6$ contains a continuous and long stretch ($\sim 200-300\mathring{A}$) with little or no detected flux to obtain more stringent limits on the neutral fraction or $J_{\rm HI}$? The idea is that since the IGM gas density naturally fluctuates spatially, it seems a priori unlikely to have no significant upward fluctuation in transmission for many pixels in a row – unless of course the neutral fraction $X_{\rm HI}$ is indeed quite high. We will show in §3.3 this provides constraints that are slightly weaker to those obtained using the mean transmission.

In all the simulations discussed in this paper, the ionizing background is assumed uniform spatially, just as in the majority of high redshift IGM simulations. A natural worry is that as the universe becomes more neutral at higher redshifts, the ionizing background would be more non-uniform. One way to test this is to use several lines of sight, available at $z \sim 5.5$, and compare the observed line-of-sight scatter in mean

[1] This part of the calculation involving the matching of the mean Lyα transmission is also similar to a number of earlier papers where the primary quantity of interest is the baryon density (e.g. Rauch et al. 1997, Weinberg et al. 1997, Choudhury et al. 2000, Hui et al. 2001). Here, we fix the baryon density and study the ionizing background or the neutral fraction instead (see §2).

transmission against the predicted scatter based on simulations with a uniform background. We discuss this in §4, estimate the level of ionizing background fluctuations, and make predictions for the scatter at $z \sim 6$. Here, we also introduce a technique to handle the problem of limited box-size.

Readers who are not interested in details can skip to §5 where we summarize the constraints obtained. We also discuss in §5 the issue of continuum placement, and how the associated uncertainties can be estimated. While the work described in this paper was being carried out, several papers appeared which investigate related issues (Barkana 2001, Razoumov et al. 2001, Cen & McDonald 2001, Gnedin 2001, Fan et al. 2001b). Where there is overlap, our results are in broad agreement with these papers. We present a comparision with other authors at the end of §3.2. Our approach here is most similar to that of Cen & McDonald (2001). In addition to obtaining constraints on the ionizing background from the Lyα and Lyβ transmission as was considered by Cen & McDonald, we consider the possible constraint from the Gunn-Peterson trough itself, examine the dependence on power spectrum normalization, and develop a method to predict the scatter in mean transmission by relating it to the power spectrum, which might be of wider interest. We also place a slightly stronger emphasis on the neutral fraction, which is more robustly determined compared to the ionizing background or photoionization rate.

2. The Gravitational Instability Model for the IGM

The Lyα optical depth is related to the IGM density, assuming ionization equilibrium , via

$$\tau_\alpha = A_\alpha (1+\delta)^{2-0.7(\gamma-1)} \tag{1}$$

where δ is the gas overdensity ($\delta = (\rho - \bar{\rho})/\bar{\rho}$, where ρ is the gas density and $\bar{\rho}$ its mean), γ is the equation of state index for the IGM[2], and A_α is given by (see e.g. Hui et al. 2001 and references therein):

$$A_\alpha = 51 \left[\frac{X_{\rm HI}}{1.6\times10^{-4}}\right]\left[\frac{\Omega_b h^2}{0.02}\right]\left[\frac{0.65}{h}\right]\left[\frac{1+z}{7}\right]^3\left[\frac{11.7}{H(z)/H_0}\right] \tag{2}$$

where $X_{\rm HI} \equiv n_{\rm HI}/n_{\rm H}$ ($n_{\rm H}$ is the total density of neutral and ionized hydrogen, and $n_{\rm HI}$ is the neutral hydrogen density) is the neutral hydrogen fraction at mean density ($\delta = 0$). [3] Here $H(z)$ is the Hubble parameter at redshift z, H_0 is the Hubble parameter today, $H_0 = 100h$ km/s/Mpc, Ω_b is the baryon density in units of the critical density. The value of 11.7 for $H(z)/H_0$ above corresponds to that appropriate for a cosmology with $\Omega_m = 0.4$ and $\Omega_\Lambda = 0.6$ at $z = 6$, where Ω_m and Ω_Λ are the matter and vacuum densities in units of the critical density today.

[2]The photoionized IGM at overdensity of a few or less is expected to follow a tight temperature-density relation of the form $T = T_0(1+\delta)^{\gamma-1}$, where T is the gas temperature and T_0 is its value at the cosmic mean density (see Hui & Gnedin 1997). We caution that close to reionization, these quantities may not be a function of δ alone. The IGM may be heated inhomogenously, causing spatial fluctuations in T_0 and γ.

[3]The neutral fraction at arbitrary δ is given by $X_{\rm HI}$ times $(1+\delta)^{1-0.7(\gamma-1)}$. Throughout this paper, whenever we quote values for $X_{\rm HI}$, we refer to the neutral hydrogen fraction at the cosmic mean density $\delta = 0$.

The neutral fraction $X_{\rm HI}$ is related to the ionizing background by [4]

$$X_{\rm HI} = 1.6 \times 10^{-4} \left[\frac{\Omega_b h^2}{0.02}\right] \left[\frac{2.55 \times 10^{-2}}{J_{\rm HI}}\right] \left[\frac{T_0}{2 \times 10^4\,{\rm K}}\right]^{-0.7} \left[\frac{1+z}{7}\right]^3 \tag{3}$$

where the dimensionless quantity $J_{\rm HI}$ is related to the photoionization rate $\Gamma_{\rm HI}$ by

$$\Gamma_{\rm HI} = 4.3 \times 10^{-12} J_{\rm HI}\,{\rm s}^{-1} \tag{4}$$

The quantity $J_{\rm HI}$ provides a convenient way of describing the normalization of the ionizing background, without specifying the exact spectrum, in a way that is directly related to the physically relevant $\Gamma_{\rm HI}$ (e.g. Miralda-Escudé et al. 1996). It is related to the specific intensity at $912\mathring{A}$ $j_{\nu_{\rm HI}}$ by $J_{\rm HI} = j_{\nu_{\rm HI}} \times [3/(\beta+3)]$, where β is the slope of the specific intensity just blueward of $912\mathring{A}$ ($j_\nu \propto \nu^{-\beta}$ where ν is frequency), and $j_{\nu_{\rm HI}}$ is measured in the customary units of $10^{-21}\,{\rm erg\,s^{-1}\,cm^{-2}\,Hz^{-1}\,ster^{-1}}$ (for non-power law j_ν, eq. [4] provides the exact definition for $J_{\rm HI}$; see e.g. Hui et al. 2001).

Two more ingredients should be mentioned to complete the specification of our model for the Lyα absorption (see e.g. Hui et al. 1997 for details). First, the optical depth as a function of velocity is computed by taking the right hand side of eq. (1) in velocity space (i.e. taking into account peculiar velocities) and smoothing it with a thermal broadening window. Second, the gas density and velocity fields are predicted by some Cold Dark Matter (CDM) cosmological model using numerical simulations.

There are obviously a number of free parameters in our model. Let us discuss each of them in turn.

Throughout this paper, we assume $\Omega_b h^2 = 0.02$, as supported by recent cosmic microwave background measurements (Netterfield et al. 2001, Pryke et al. 2001) and the nucleosynthesis constraint from primordial deuterium abundance (Burles et al. 2001). We also assume throughout $h = 0.65$, $\Omega_m = 0.4$, and $\Omega_\Lambda = 0.6$. Variations of these parameters within the current bounds do not contribute significantly to the uncertainties of the constraints obtained in this paper (see Hui et al. 2001).

The temperature T_0 and equation of state index γ at the redshifts of interest in this paper are somewhat uncertain. There are no direct measurements of the thermal state of the IGM at our redshifts of interest, $z \gtrsim 4$. Measurements at $z \lesssim 4$ yield values consistent with $T_0 = 2 \times 10^4$ K and $\gamma = 1$ (McDonald et al. 2000b, Ricotti et al. 2000, Zaldarriaga et al. 2001. Schaye et al. 2000, however, measure a slightly lower temperature). Given that the temperature right after reionization is expected to be about 25000 K with $\gamma = 1$ (with some dependence on the hardness of the ionizing spectrum; see e.g. Hui & Gnedin 1997), which is not too different from the measurements at $z \lesssim 4$, we will assume throughout this paper, when making use of eq. (3) to infer $J_{\rm HI}$, that $T_0 = 2 \times 10^4$ K and $\gamma = 1$. Note that while the theoretically allowed range for γ is from 1 to 1.6 (Hui & Gnedin 1997), what matters for our purpose is $2 - 0.7(\gamma - 1)$ (eq. [1]), which only ranges from 1.58 to 2, and does not significantly affect our results. It is also important to emphasize that *the inference of $X_{\rm HI}$ from observations, unlike the case for $J_{\rm HI}$, is not subject directly to uncertainties in the temperature T_0*. This is because observations constrain A_α from which we can obtain $X_{\rm HI}$ without knowing T_0 (see eq. [2]). [5]

[4]This equation assumes that hydrogen is highly ionized and that helium is largely doubly ionized. If helium is only singly ionized, the relation between $J_{\rm HI}$ and $X_{\rm HI}$ will be changed slightly: the right hand side of eq (3) will be multiplied by 0.93.

[5] The above statement is subject to two small caveats. First, the optical depth given in eq. (1) has to be smoothed with a thermal broadening window whose width depends on T_0. We find that in practice, the exact width of the thermal broadening kernel does not affect very much quantities such as the mean transmission, which is what we will be interested in. Second, T_0 also affects the gas dynamics via the pressure term in the equation of motion. As we will discuss below, the effect of varying T_0 also appears to be small in this regard.

To generate realizations of the density and velocity fields for a given cosmology, we run Hydro-Particle-Mesh (HPM) simulations (Gnedin & Hui 1998). The HPM algorithm is essentially a Particle-Mesh code, modified to incorporate a force term due to gas pressure in the equation of motion. [6] For the initial power spectrum, we use a Cold Dark Matter (CDM) type transfer function, as parameterized by Ma (1996), which is very similar to the commonly used Bardeen et al. (1986) transfer function. For the primordial spectral slope, we adopt $n = 0.93$ (Croft et al. 2000, McDonald et al. 2000a). For the linear power spectrum normalization, we employ the range suggested by measurements from the Lyα forest of Croft et al. (2000): $\Delta^2(k) \equiv 4\pi k^3 P(k)/(2\pi)^3 = 0.74^{+0.20}_{-0.16}$ at $z = 2.72$ at a velocity scale of $k = 0.03(\,\mathrm{km/s})^{-1}$.[7] We, however, caution that the error-bar given is somewhat dependent on the assumed error of the mean transmission measurements, which is sensitive to the accuracy of the continuum-fitting procedure (see e.g. Zaldarriaga et al. 2001 for a slightly different assessment of the error-bar). The power spectrum in this model has a similar shape to that of favored cosmological models, but slightly lower amplitude (Croft et al. 2000). In §3.2 we demonstrate that our main conclusion, that the neutral fraction increases dramatically near $z \sim 6$, is insensitive to our assumptions about the amplitude of the power spectrum. In practice, we examine models with different normalizations by running a simulation with outputs at several different redshifts: each redshift then corresponds to a different power spectrum normalization, and linear interpolation is performed to reach any desired normalization. [8]

Our simulations have a box size of 8.9 Mpc/h, with a 256^3 grid. McDonald & Miralda-Escude (2001) found this box size and resolution to be adequate for IGM studies up to $z \sim 5$. We have verified that the same is true up to $z = 6$, in the sense that the transmission probability distribution has converged for our choice of simulation size and resolution.

Finally, we should say a few words about simulations of the Lyβ region. In regions of the quasar spectrum that are between $973\mathring{A}(1 + z_{\mathrm{em.}})$ and $1026\mathring{A}(1 + z_{\mathrm{em.}})$, where $z_{\mathrm{em.}}$ is the redshift of the quasar, two kinds of absorption can exist: one is Lyβ due to material at redshift $0.948(1 + z_{\mathrm{em.}}) < 1 + z < 1 + z_{\mathrm{em.}}$, the other is Ly$\alpha$ due to material at redshift $0.800(1 + z_{\mathrm{em.}}) < 1 + z < 0.844(1 + z_{\mathrm{em.}})$. In other words, in such a region, the observed optical depth would be given by $\tau = \tau_\beta + \tau_\alpha$ where τ_β and τ_α arises at different redshifts. The Lyα optical depth can be computed as before. The Lyβ optical depth τ_β can be computed using eq. (1), except that A_α is replaced by A_β:

$$A_\beta = \frac{1}{5.27} A_\alpha \tag{5}$$

The factor of 5.27 reflects the fact that the Lyβ transition has a cross-section that is 5.27 times smaller than Lyα.

---

[6] The temperature-density relation has to be specified as a function of redshift in the HPM code to compute the pressure term. We follow McDonald & Miralda-Escudé (2001) and linearly interpolate between $T_0 = 19000$ K and $\gamma = 1.2$ at $z = 3.9$ and $T_0 = 25000$ K and $\gamma = 1$ at the redshift of reionization z_{reion}. We found that assuming $z_{\mathrm{reion}} = 7$ versus $z_{\mathrm{reion}} = 10$ results in negligible difference in our results, in particular concerning the mean decrement and the probability distribution of transmission. All results in this paper are quoted from the $z_{\mathrm{reion}} = 7$ HPM simulations. Note that in inferring X_{HI} and J_{HI} from eq. (2) and (3), we always use $T_0 = 20000$ K and $\gamma = 1$ for simplicity, as mentioned before.

[7] This normalization corrects an error in an earlier draft of Croft et al. (2000). (R. Croft, private communication.)

[8] We do not vary the primordial spectral index n here. Quantities such as the mean transmission which we are interested in here are generally sensitive to power on only a small range of scales. Varying n is therefore largely degenerate with varying Δ^2.

3. Constraints on the Neutral Hydrogen Fraction and the Ionizing Background

3.1. Constraints from the Lyα Mean Transmission

Using eq. (1) and (2), we compute the $X_{\rm HI}$, which also fixes $J_{\rm HI}$ (eq. [3]), necessary to match the observed Lyα mean transmission $\langle e^{-\tau_\alpha}\rangle$ at $z = 4.5 - 6$ (see Table 1 for a summary of the measurements). The results of our calculation are presented in Fig. 1. This plot also contains a point at $z = 6.05$ which is the result of matching the mean transmission in the Lyβ forest, as we describe in §3.2.

Also shown in the figure is a dotted line which shows $X_{\rm HI} \propto (1+z)^3$, which appears to be a good fit to the data from $z = 4.5$ to $z = 5.7$. From eq. (3), one can see that such a trend for the neutral fraction is equivalent to assuming constant $J_{\rm HI}$ (or more accurately, constant $J_{\rm HI}T_0^{0.7}$; see eq. [3]).

As one can see, ignoring for now the Lyβ point, the neutral fraction does appear to have a modest jump around $z \sim 6$: it increases by a factor of ~ 4.0 from $z = 5.7$ to $z = 6.05$, while it changes at most by ~ 1.9 from $z = 4.5$ to $z = 5.7$. A similar trend (but opposite in sign) can be seen in the ionizing flux $J_{\rm HI}$. The 1 σ error-bar here takes into account the measurement error in mean transmission, and the range of power spectrum normalization stated in §2. As we have explained in §2, while $X_{\rm HI}$ is not sensitive to the assumed temperature of the IGM (T_0), our constraints on $J_{\rm HI}$ are directly influenced by it. As emphasized before, we assume $T_0 = 2 \times 10^4$ K. In other words, our constraints on $J_{\rm HI}$ are really constraints on the quantity $J_{\rm HI}(T_0/2\times 10^4\,{\rm K})^{0.7}$ (see eq. [3]). It is therefore straightforward to rescale our constraints on $J_{\rm HI}$ if the temperature were a little bit different. [9] It is an interesting question to ask whether the apparent jump in the ionizing flux can instead be attributed to a jump in the temperature. In general, the temperature is expected to evolve slowly with redshift after reionization (Hui & Gnedin 1997).

Regarding the measurement error, we should also emphasize that the Becker et al.'s 2 σ error actually includes the possibility of having zero transmission at $z = 6.05$. This means that at 2 σ, we would only have a lower limit on $X_{\rm HI}$, or an upper limit on $J_{\rm HI}$, for the highest redshift point in Fig. 1, allowing the possibility that the IGM is neutral at $z \sim 6$, $X_{\rm HI} = 1$.

3.2. Constraints from the Lyβ Mean Transmission

In this section we consider the constraints placed by Becker et al.'s measurement of the mean transmission in the Lyβ region. Absorption in the Lyβ region has two components: $\tau = \tau_\alpha + \tau_\beta$, where the Ly$\alpha$ optical τ_α and the Lyβ optical depth τ_β originate at different redshifts. Lyβ absorption due to material at $z = 6$ coincides in wavelength with Lyα absorption due to material at $z = (1+6)\times 1026/1216 - 1 = 4.9$. Because the points of origin are so widely separated, they can be effectively treated as statistically independent i.e. $\langle e^{-\tau}\rangle = \langle e^{-\tau_\alpha}\rangle\langle e^{-\tau_\beta}\rangle$. Becker et al. measured $\langle e^{-\tau_\beta}\rangle$ at $z \sim 6$ by dividing the net mean transmission $\langle e^{-\tau}\rangle$ in the Lyβ region by the mean transmission in Lyα at $z \sim 5$. They obtained $\langle e^{-\tau_\beta}\rangle = -0.002 \pm 0.020$. Clearly, this measurement is consistent with a completely neutral IGM. However, the interesting question is: what kind of lower limit does it set on the neutral fraction, and does it improve upon the lower limit from the mean Lyα absorption ?

We carry out a calculation that is analogous to what is described in §3.1, except for the key difference

[9] The temperature also affects the thermal broadening window, but we find that in practice its effect on our constraints on A_α (eq. [2]) is small; see discussion in §2.

that in computing τ_β from the simulated density and velocity fields, we employ A_β which is a factor of 5.27 smaller than A_α (see eq. [1] & [5]). The results of our calculation are shown in Fig. 1, as the highest redshift points in the plot, which have error bar arrows pointing towards a completely neutral IGM and a vanishing ionizing background. It can be seen that the $(1-\sigma)$ lower limit on $X_{\rm HI}$ is $X_{\rm HI} > 4.7 \times 10^{-4}$. This is a factor of ~ 3 larger than the neutral fraction required to match the upper limit on the mean transmission in Lyα for our fiducial normalization, and a slightly stronger constraint than that obtained in section 3.1, including the uncertainty in power spectrum normalization. Similarly, the upper limit on $J_{\rm HI}$ is $J_{\rm HI} < 9.0 \times 10^{-3}$. The moral here is that because the Lyβ absorption cross-section is a factor of 5.27 smaller than the Lyα cross-section, Lyβ offers a more sensitive probe of the neutral fraction, especially when the Lyα optical depth is high.

The neutral fraction at $z \sim 6$ is thus a factor of ~ 10 higher than that at redshift $z \sim 5.7$, where it is $X_{\rm HI} = 4.9 \times 10^{-5}$. This dramatic change in the neutral fraction is suggestive, probably indicating that the reionization epoch is nearby.

Furthermore, this conclusion is not sensitive to our assumptions about the amplitude of the power spectrum. Although the neutral fraction at redshift $z = 6.05$ is itself sensitive to the amplitude of the power spectrum, we find that the factor by which the neutral fraction increases from $z = 5.7$ to $z = 6.05$ depends only weakly on the amplitude. In Fig. 2 we plot both the neutral fraction at $z = 6.05$ and the jump in the neutral fraction for a range of different power spectrum normalizations. The jump is defined as the ratio $X_{\rm HI}(z = 6.05)/X_{\rm HI}(z = 5.7)$. Here $X_{\rm HI}(z = 6.05)$ is the lower limit resulting from the 1 σ error in the mean transmission in Lyβ at $z = 6.05$ and the error bars in the jump arise from the 1 σ error in the mean transmission in Lyα at $z = 5.7$. As one can see in the plot, the lower limit on the neutral fraction at $z = 6.05$ varies from $X_{\rm HI} > 3 \times 10^{-4}$ to $X_{\rm HI} > 9 \times 10^{-4}$ as $\Delta^2(k = 0.03(\,{\rm km/s})^{-1}, z = 2.72)$ varies from 0.5 to 1.3. The neutral fraction itself varies significantly with power spectrum normalization, scaling approximately as $X_{\rm HI} \propto [\Delta^2(k = 0.03\,{\rm s/km}, z = 2.72)]^{1.1}$, for this range of normalizations. The jump, however, changes only slightly over a large range of normalizations. As $\Delta^2(k = 0.03(\,{\rm km/s})^{-1}, z = 2.72)$ varies from 0.5 to 1.3, the jump changes only from ~ 9.7 to ~ 11.1. Our conclusion that the neutral fraction of the IGM increases dramatically near $z \sim 6$ seems robust.

One can also consider the absorption in the Lyγ region, or even the higher Lyman series. In practice, the accumulated amount of absorption from Lyα as well as Lyβ at different redshifts makes it harder to measure the Lyγ transmission itself with good accuracy.

Our constraints on the neutral fraction and the intensity of the ionizing background are consistent with those found by other authors, given our different choices of power spectrum normalization. Fan et al. (2001b) found, from the mean Lyβ transmission, that $\Gamma_{-12} < 0.025$, where Γ_{-12} is the photoionization rate of eq (4) in units of $10^{-12}\,{\rm s}^{-1}$. Although this constraint is somewhat stronger than the constraint implied by our fiducial model, $\Gamma_{-12} < 0.039$, we expect the difference due to our different power spectrum normalizations. Fan et al.'s (2001b) constraint comes from semi-analytic arguments, shown consistent with an LCDM simulation with $\Omega_m = 0.3$, $\Omega_\Lambda = 0.7$,$h = 0.65$, $\Omega_b h^2 = 0.02$, and $\sigma_8 = 0.9$. This model has a substantially larger normalization, $\Delta^2(k = 0.03(\,{\rm km/s})^{-1}, z = 2.72) = 1.25$, than our fiducial model of $\Delta^2(k = 0.03(\,{\rm km/s})^{-1}, z = 2.72) = 0.74$. The difference in normalization reflects some tension between the normalization derived from the observed cluster abundance, which Fan uses, and that from the Lyman-α forest which our model is based on (Croft et al. 2000). Fan et al. (2001b) assume $T_0 = 2.0 \times 10^4$ K in placing their constraint. Their limit, $\Gamma_{-12} < 0.025$, includes only uncertainties in the mean transmission and not additional uncertainties from the power spectrum normalization. From figure (2), we infer that Fan et al.'s (2001b) normalization implies $X_{\rm HI} > 8.8 \times 10^{-4}$ in our cosmology. Rescaling this result from our

assumed $\Omega_m = 0.4$ to an $\Omega_m = 0.3$ cosmology, and using eqs. (3) and (4) we predict $\Gamma_{-12} < 0.024$, or $X_{\rm HI} > 7.6 \times 10^{-4}$, for Fan et al.'s (2001b) model. The constraint of Fan et al. (2001b) is thus consistent with our constraint given our different choice of normalization. Cen & McDonald (2001), using a model similar to that of Fan et al. (2001b), obtained the constraint $\Gamma_{-12} < 0.032$, using the Lyβ mean transmission. The constraint is slightly weaker than that of Fan et al. (2001b) and our extrapolation to their normalization, because Cen & McDonald (2001) consider a larger upper limit to the observed mean transmission, including an estimate of the uncertainty due to sky subtraction. At slightly lower redshifts, we can also compare with the results of McDonald & Miralda-Escudé (2001) derived from matching the mean Lyα transmission. For example, at $z = 5.2$, these authors found $\Gamma_{-12} = 0.16$ to match the observed mean transmission of $\langle e^{-\tau_\beta} \rangle = 0.09$. McDonald & Miralda-Escudé (2001) consider a model whose normalization we infer to be $\Delta^2(k = 0.03(\,{\rm km/s})^{-1}, z = 2.72) = 0.98$. To match the same mean transmission with this normalization we infer a somewhat higher photoionization rate, $\Gamma_{-12} = 0.19$. Part of the difference may be that the Γ_{-12} necessary to match a given mean transmission varies by $\sim 5\%$ between two different realizations of the density field. The remaining difference may come from the procedure of linearly interpolating between outputs or from some modeling difference. At any rate, our results are roughly consistent with those of other authors given our different power spectrum normalizations.

3.3. Constraints from the Gunn-Peterson Trough Itself – the Fluctuation Method

The fact that Becker et al. (2001) observed a Gunn-Peterson trough, where a long stretch of the spectrum contains little or no flux, can conceivably be used to further tighten the constraints obtained from the previous sections. Since the IGM is expected to have spatial fluctuations, the probability of having many pixels in a row turning up a very small transmission must be low, unless the neutral fraction is intrinsically quite high. The same reasoning can be applied to either the Lyα or Lyβ absorption. We will discuss our method for Lyα in detail. The method for Lyβ is a straightforward extension. For simplicity, we will call this method, the fluctuation method.

Becker et al. (2001) finds from the spectrum of SDSS 1030+0524, the $z = 6.28$ quasar, the Lyα transmission is consistently below about 0.06 for a region that spans $260\mathring{A}$, between $8450\mathring{A}$ to $8710\mathring{A}$. The noise level per $4\mathring{A}$ pixel is $\sqrt{\langle n^2 \rangle} \sim 0.02$, where n represents the photon noise fluctuation. [10] The observed transmission F at a given pixel is $F = e^{-\tau} + n$, where $e^{-\tau}$ is the true transmission. The noise here should be dominated by Poisson fluctuations of the subtracted sky background (as well as perhaps read-out error). Let $P(F_1, F_2, ...F_N)dF_1...dF_N$ be the probability that N consecutive pixels have observed transmission fall into the range $F_1 \pm dF_1/2$ ... $F_N \pm dF_N/2$. In our case, $N = 65$ for the pixel size of $4\mathring{A}$. The problem is then to find the probability $\int_{<0.06} ... \int_{<0.06} P(F_1...F_N)dF_1...dF_N$ as a function of $J_{\rm HI}$, and ask what maximal $J_{\rm HI}$ (or equivalently, minimal $X_{\rm HI}$) would give an acceptable probability. By choosing the "acceptable probability" to be within 68% of the maximum likelihood (maximum likelihood is achieved when the neutral fraction is unity), we obtain the 1 σ upper limit on $J_{\rm HI}$ or 1 σ lower limit on $X_{\rm HI}$.

Our simulation has a comoving box size of 8.9 Mpc/h, corresponding to $42\mathring{A}$ for Lyα at $z \sim 6$, which falls short of the wavelength range we need for this problem, which is $260\mathring{A}$. In other words, the probability

[10] We estimate the noise per pixel from Becker et al.'s error-bar in the mean transmission, which is ~ 0.003. This is estimated from a chunk of the spectrum which is $260\mathring{A}$ long, and so the dispersion per $4\mathring{A}$ pixel should be approximately $\sqrt{\langle n^2 \rangle} \sim 0.003 \times \sqrt{65} \sim 0.02$. Note that the actual dispersion varies across the spectrum, but this should suffice as a rough estimate. This estimate also agrees with an estimate of the error by comparing Fig. 1 and Fig. 3 of Becker et al.

$P(F_1, F_2, ...F_N)dF_1...dF_N$ can be estimated directly from our simulation only for $N \leq 10$. However, the mass correlation length scale at this redshift ($\lesssim 1$ Mpc/h) is actually a fraction of the box size, which means one can treat fluctuations on scales beyond the box size as roughly uncorrelated. Assuming so, we estimate $\int_{<0.06} ... \int_{<0.06} P(F_1, F_2, ...F_{10})dF_1...dF_{10}$ from the simulation, and then take its 6-th power, which would give us the probability that 60 consecutive pixels have transmission below 0.06. This is slightly smaller than the number 65 that we need, but at least will provide us conservative constraints on $X_{\rm HI}$ and $J_{\rm HI}$. We have also tested our approach by using fractions of the box-size as a unit, and find that our results do not change significantly (less than 10%).

Fig. 3a (dotted curve) shows our estimate of the probability $\int_{<0.06} ... \int_{<0.06} P(F_1, F_2, ...F_N)dF_1...dF_N$ for $N = 60$ and pixel size $4\mathring{A}$, as a function of $J_{\rm HI}$. Our simulated spectra have been convolved with the observation resolution (full-width-at-half-maximum of $1.8\mathring{A}$), rebinned into pixels of $4\mathring{A}$ each and added Gaussian noise with a dispersion of 0.02. From the dotted curve in Fig. 3a, applying a likelihood analysis, we obtain a 1 σ upper limit on $J_{\rm HI}$ of $J_{\rm HI} < 0.014$, and a corresponding lower limit on $X_{\rm HI}$ of $X_{\rm HI} > 2.95 \times 10^{-4}$. This is for a model with a power spectrum normalization of $\Delta^2(k = 0.03\,{\rm s/km}, z = 2.72) = 0.74$ (see §2). The mean Lyα transmission constraints for the same model are $J_{\rm HI} < 0.028$ and $X_{\rm HI} > 1.5 \times 10^{-4}$. [11] *This means that considering Lyα alone, the fluctuation method yields somewhat stronger constraints compared to using simply the mean transmission.*

Fig. 3b (dotted curve) shows the same methodology applied to the Lyβ Gunn-Peterson trough. A new ingredient here is that one needs an additional simulation of the same model at redshift $z = 4.9$ to produce the Lyα absorption that can be overlaid on top of the Lyβ absorption from $z = 6.05$. This additional simulation should have different initial phases to mimic the fact that fluctuations at $z = 4.9$ and those at $z = 6.05$ should be uncorrelated. We obtain 1 σ limits of $J_{\rm HI} < 0.012$ and $X_{\rm HI} > 3.4 \times 10^{-4}$. This is about 40% weaker than the constraints we obtain from the Lyβ mean transmission. *In other words, from Lyβ absorption, the fluctuation method yields slightly weaker constraints compared to using the mean transmission.* It is also only slightly stronger than the constraint obtained from the fluctuation method applied to Lyα.

It is an interesting question to ask how many sightlines one would need to improve the constraints by, say a factor of 2. Our approach can be easily extended to multiple (uncorrelated) sightlines, and we find that about 5 sightlines (each containing a Gunn-Peterson trough of the same length and same signal to noise) are necessary for such an improvement.

Part of the difficulty with obtaining stronger constraints, in addition to the small number of sightlines, is the dominance of noise. The lower panel of Fig. 4 shows the one-pixel ($4\mathring{A}$) probability distribution function (PDF) of the true transmission $e^{-\tau}$ (i.e. no noise added), for three different values of $J_{\rm HI}$ (the power spectrum normalization is the same as that in Fig. 3). The upper panel shows the corresponding PDF's of the observed transmission F (i.e. after convolving $P(e^{-\tau})$ with a Gaussian of dispersion 0.02). As expected, noisy data make the PDF's more similar. Nonetheless, as we pointed out above, with sufficient number of sightlines, there might be a non-negligible chance of seeing pixels with high transmission that take place at the tail of the PDF's, hence allowing us to distinguish between the different levels of the ionizing background. Alternatively, one can try improving the signal-to-noise per pixel. In Fig. 3b, we show with a dashed curve the corresponding probability if the noise per pixel is lowered by a factor of 4. The constraints improve by a little more than a factor of 2. We should emphasize, however, systematic errors are likely

[11] Do not confuse these constraints, which are for the particular power spectrum normalization mentioned above, to the constraints discussed in earlier sections, which include the uncertainty in the power spectrum normalization. We focus on a single model in this section for simplicity.

important here – we will discuss them in the next two sections.

4. The Variance of the Mean Transmission

If, as is suggested by our discussion in §3.2 (see Fig. 1), the IGM is close to the epoch of reionization at $z \sim 6$, one might expect large fluctuations in the ionizing background near that time. For instance, one line of sight might probe a region of the IGM where the ionized bubbles around galaxies or quasars have percolated, while another might probe the pre-percolation IGM. As mentioned before, the simulations we employ do not take into account fluctuations in the ionizing background. (For simulations incorporating radiative transfer see e.g., Gnedin & Abel 2001, Razoumov 2001). One useful check would then be to predict the sightline to sightline scatter in mean transmission from our simulations, and compare that against the observed scatter. At $z \sim 5.5$, 4 lines of sight are available for a measurement of the scatter. We will examine this, as well as make predictions for the scatter at $z \sim 6$, which more high redshift quasars in the future will allow us to measure.

Our estimate relies on simulation measurements of the transmission power spectrum. This is in contrast to an estimate of the same quantity made by Zuo (Zuo 1993) who makes a prediction based on extrapolations of the column density distribution and of the number of absorbing clouds per. unit redshift (Zuo & Phinney 1993). Zuo also assumes that the clouds are Poisson distributed, while our measurement incorporates the clustering in the IGM via our numerical simulation.

An immediate problem presents itself: sightlines from which the mean transmission is measured are typically longer than the usual simulation box. We tackle this problem by expressing the variance of mean transmission in terms of the transmission power spectrum, and making use of a reasonable assumption about the behavior of the power spectrum on large scales.

The mean transmission from one sightline is estimated using

$$\bar{F} = \frac{1}{N}\sum_{i=1}^{N} F_i \tag{6}$$

where N is the number of pixels, F_i is the observed transmission at pixel i, $F_i = f_i + n_i$ where $f = e^{-\tau}$ is the true transmission and n is the noise fluctuation. We use the symbol $\bar{F}$ to represent the estimator, and $\bar{f}$ to denote the true mean transmission. The variance of the estimated mean transmission is then

$$\sigma_T^2 \equiv \langle \bar{F}^2 \rangle - \langle \bar{F} \rangle^2 = \frac{1}{N^2}\sum_{i,j}[\langle F_i F_j \rangle - \langle F_i \rangle \langle F_j \rangle] \tag{7}$$

$$= \frac{1}{N^2}\sum_{i,j}\xi_{ij} + \frac{1}{N}\sigma_n^2 = 2\int_0^\infty \frac{dk}{2\pi}\left[\frac{\sin(kL/2)}{kL/2}\right]^2 P_f(k) + \frac{\sigma_n^2}{N}$$

where $\sigma_n^2 \equiv \langle n^2 \rangle$ is assumed roughly independent of position, and ξ_{ij} is the un-normalized two-point correlation of the transmission i.e. $\xi_{ij} \equiv \langle f_i f_j \rangle - \bar{f}^2$, and $P_f(k)$ is its one-dimensional Fourier transform. The symbol L denotes the comoving length of the spectrum from which the mean transmission is measured, and k is the comoving wavenumber.

To evaluate σ_T, we need to know the transmission power spectrum on scales generally larger than the size of the typical simulation box. It is expected that the transmission power spectrum takes the shape (not the normalization) of the linear mass power spectrum on large scales (i.e. essentially linear

biasing; see Scherrer & Weinberg 1998, Croft et al. 1997, Hui 1999). We therefore use this to extrapolate the simulation $P_f(k)$ to large scales (small k's). We find that $P_f(k)$ is well approximated by $P_f(k) = B\exp(-ak^2)\int_k^\infty (dk/2\pi)kP_{\rm mass}(k)$ where $P_{\rm mass}$ is the three-dimensional linear mass power spectrum.

Becker et al. gave an estimate of $\sigma_T \sim 0.03 \pm 0.01$, $\bar{f} = 0.1$, at $z = 5.5$ using 4 different sightlines, each spanning $\Delta z = 0.2$, which corresponds to $L \sim 57$ Mpc/h. [12] An estimate of the noise term is provided by the error in the mean transmission, $(\sigma_n^2/N)^{0.5} \sim 0.003$. For the $\Delta^2(k = 0.03\,{\rm s/km}, z = 2.72) = 0.74$ case, the fitting parameters are $B = 0.033$ and $a = 0.013\,{\rm Mpc^2/h^2}$. Using eq. (5), we then find $\sigma_T = 0.030$ for $\Delta^2(k = 0.03\,{\rm s/km}, z = 2.72) = 0.74$, $\sigma_T = 0.031$ for $\Delta^2(k = 0.03\,{\rm s/km}, z = 2.72) = 0.94$, and $\sigma_T = 0.028$ for $\Delta^2(k = 0.03\,{\rm s/km}, z = 2.72) = 0.58$. The variance is similar between the different normalizations because each normalization requires a different A_α in eq. (1) to match the mean transmission. This difference in A_α probably compensates for the effect of the different normalizations on σ_T. The predicted scatter of $\sigma_T \sim 0.030$ is consistent with the measured σ_T of 0.03 ± 0.01.

We apply the same methodology as the above to estimate σ_T at $z \sim 6$. In Fig. 5, we show the results for a range of different $J_{\rm HI}$'s for each of our canonical power spectrum normalizations, ($\Delta^2(k = 0.03\,{\rm s/km}, z = 2.72) = 0.58, 0.74$ and 0.94). [13] Photon noise is not included in the estimates of this figure. Even for relatively large $J_{\rm HI}$'s the scatter is small. For instance, for $J_{\rm HI} = 4.5 \times 10^{-2}$, $\sigma_T = 1.1 \times 10^{-2}$, assuming our fiducial normalization. This $J_{\rm HI}$ is large in that it already gives a mean transmission, $\bar{f} = 1.75 \times 10^{-2}$, in excess of the observations. By $J_{\rm HI} = 1.4 \times 10^{-2}$, the scatter is only $\sigma_T = 2.8 \times 10^{-3}$ for our fiducial normalization. The scatter depends somewhat on normalization, as one can see in the figure. To measure the scatter well would require data that are less noisy than the one discussed here, which has photon noise of $(\sigma_n^2/N)^{0.5} \sim 0.003$, comparable to the predicted scatter.

On the other hand, the smallness of this scatter makes it a possibly interesting diagnostic. As we have emphasized before, this predicted scatter ignores fluctuations in the ionizing background. For sufficiently small $J_{\rm HI}$'s, the IGM should be close to the epoch of reionization, and one would expect large sightline by sightline variations. An observed scatter well in excess of what is predicted would be an interesting signature.

5. Discussion

Our findings are summarized as follows.

- The most stringent ($1\,\sigma$) lower limit on the neutral hydrogen fraction $X_{\rm HI}$ (eq. [3]) or upper limit on the ionizing background $J_{\rm HI}$ (eq. [4]) at $z \sim 6$ is obtained from the observed mean Lyβ transmission: $X_{\rm HI} > 4.7 \times 10^{-4}$. A comparison of this limit versus constraints at lower redshifts is presented in Fig. 1. The fact that the neutral fraction increases by a factor of ~ 10 from redshift of 5.7 to 6 even though it changes by no more than a factor of about 2 from $z = 4.5$ to $z = 5.7$ suggests that $z \sim 6$ might be very close to the epoch of reionization. We emphasize that current constraints are still consistent with a highly ionized IGM at $z \sim 6$ – it is the steep rise in $X_{\rm HI}$ that is suggestive of dramatic changes around

[12] The error on σ_T is estimated assuming Gaussian statistics and that the four lines of sight are independent. Then $var(\sigma_T) = \sigma_T^2/2n$ (see e.g. Kendall & Stuart 1958).

[13] The comparison across normalizations is done here at fixed $J_{\rm HI}$ while at $z = 5.5$ we compared the results of different normalizations at fixed mean transmission. We find that the dependence on normalization is larger at fixed $J_{\rm HI}$ than at fixed mean transmission.

or just before that redshift. We should also mention that the constraints on $X_{\rm HI}$ are less subject to uncertainties in the IGM temperature compared to those on $J_{\rm HI}$ (see §2).

- The existence of a long Gunn-Peterson (Lyα or Lyβ) trough at $z \sim 6$, where little or no flux is detected, can also be used to obtain constraints on $X_{\rm HI}$ or $J_{\rm HI}$. This we call the fluctuation method: the fact that a long stretch of the spectrum exhibits no large upward fluctuations in transmission provides interesting information on the neutral fraction or ionizing background. The constraints obtained this way turn out to be fairly similar to those obtained using the mean transmission. We estimate that a reduction in noise by a factor of 4, or an increase in number of sightlines to 5, would result in constraints that are 2 times stronger (§3.3).

- We develop a method to predict the dispersion in mean transmission measured from sightlines that are longer than the typical simulation box (eq. [7] and Fig. 5). Our predicted dispersion is consistent with that observed at $z = 5.5$ (Becker et al. 2001). We also predict the scatter at redshift $z = 6$, which can be measured when more sightlines become available. Assuming a spatially homogeneous ionizing background, we predict a small scatter at $z = 6$, $\sigma_T \sim$ a few $\times 10^{-3}$, neglecting photon noise. The dispersion provides a useful diagnostic of fluctuations in the ionizing background – close to the epoch of reionization, one expects large fluctuations from one line of sight to another depending on whether it goes through regions of the IGM where percolation of HII regions has occurred.

There are at least three issues that will be worth exploring. First, with more quasars at $z \sim 6$ or higher discovered in the future, applying some of the ideas mentioned above would be extremely interesting, such as the measurement of the line of sight scatter in mean transmission, or the use of the Gunn-Peterson trough to obtain stronger constraints on the neutral fraction. Second, as we have commented on before, fluctuations in the ionizing background are expected to be important as we near the epoch of reionization. We have not discussed it here, but a calculation of the size of these fluctuations would be very interesting. Such a calculation will depend both on the mean free path of the ionizing photons as well as the spatial distribution of ionizing sources. The latter is probably quite uncertain, but useful estimates might be made (e.g. Razoumov et al. 2001). Lastly, a main source of systematic error which we have not discussed is the continuum placement. The mean transmissions at various redshifts given by Becker et al. are all obtained by extrapolating the continuum from the red side of Lyα by assuming a power law of $\nu^{-0.5}$. The continuum likely fluctuates from one quasar to another, and therefore, it would be very useful to apply exactly the same procedure to quasars at lower redshifts where the continuum on the blue side can be more reliably reconstructed. This will tell us how much scatter (and possibly systematic bias) the continuum placement procedure introduces to the measured mean transmission. This kind of error is especially important to quantify given the limited number of quasars available for high redshift measurements at the moment.

AL and LH are supported in part by the Outstanding Junior Investigator Award from the DOE, and AST-0098437 grant from the NSF. MZ is supported by NSF grants AST 0098606 and PHY 0116590 and by the David and Lucille Packard Foundation Fellowship for Science and Engineering. We thank Nick Gnedin for the use of an HPM code and Rupert Croft for providing us with a revised draft of his paper.

References

Anderson, S. F. et al. 2001, AJ, 122, 503
Bardeen, J. M., Bond, J. R., Kaiser, N., & Szalay, A. S. 1986, ApJ, 304, 15
Barkana, R. 2001, submitted to New Astronomy (astro-ph 0108431)

Becker, R. H., Fan, X., White, R. L., Strauss, M. A., Narayanan, V. K., Lupton, R. H., Gunn, J. E. et al. 2001, AJ, in press (astro-ph/0108097)
Bi, H. & Davidsen, A. F., 1997, ApJ **479**, 523
Bond, J. R. & Wadsley, J. W., 1997, *Proc. 12th Kingston Conf., Halifax*, (astro-ph 9703125)
Bryan, G., Machacek, M., Anninos, P., & Norman, M. L. 1999, ApJ, 517, 13
Burles, S., Nollett, K. M., & Turner, M. S. 2001, ApJ, 552L
Cen, R., Miralda-Escudé, J., Ostriker, J. P., Rauch, M. 1994, ApJ, 437, L9
Cen, R., McDonald, P. 2001, ApJL, submitted (astro-ph 0110306)
Choudhury, T. R., Srianand, R. & Padmanabhan, T. 2000 submitted to ApJ, astro-ph 0012498
Croft, R. A. C., Weinberg, D. H., Katz, N., & Hernquist, L., 1998a, ApJ **495**, 44
Croft, R. A. C., Weinberg, D. H., Bolte, M., Burles, S., Hernquist, L., Katz, N., Kirkman, D., & Tytler, D. 2000, ApJ, submitted (astro-ph 0012324)
Djorgovski, S. G., Castro. S. M., Stern, D. & Mahabal, A. 2001, ApJL, in press (astro-ph 0108069)
Fan, X., et al. 2000, AJ, 120, 1167
Fan, X., et al. 2001a, AJ, in press (astro-ph 0108063)
Fan, X., et al. 2001b, AJ, submitted (astro-ph 0111184)
Gnedin, N. 2001, submited to MNRAS (astr-ph 0110290)
Gnedin, N, & Abel, T. 2001, New Astronomy, in press (astro-ph 0106278)
Gnedin, N., & Hui, L. 1998, MNRAS, 296, 44
Gunn, J. E., & Peterson, B. A. 1965, ApJ, 142, 1633
Haehnelt, M. G., Madau. P., Kudritzki, R. P., Haardt, F., 2000, ApJ, in press (astro-ph 0010631)
Hernquist, L., Katz, N., Weinberg, D. H., & Miralda-Escudé, J., 1996, ApJ 457, L51
Hui, L. & Gnedin, N. Y., 1997, MNRAS 292, 27
Hui, L., Gnedin, N. Y., & Zhang, Y., 1997, ApJ 486, 599
Hui, L., 1999, ApJ, 516, 519
Hui, L., Haiman, Z., Zaldarriaga, M., & Alexander, T. 2001, ApJ, in press (astro-ph 0104442)
Kendall, M. G., & Stuart, A. 1958, The Advanced Theory of Statistics, v. 1, (New York: Hafner)
Ma, C.-P., 1996, ApJ, 471, 13
McDonald, P., Miralda-Escudé, J., Rauch, M., Sargent, W. L. W., Barlow, T. A., Cen, R., & Ostriker, J. P., 2000a, ApJ, 543, 1
McDonald, P., Miralda-Escudé, J., Rauch, M., Sargent, W. L. W., Barlow T. A., Cen R., & Ostriker, J. P., 2000b, ApJ, submitted (astro-ph 0005553)
McDonald, P. & Miralda-Escudé, J., 2001, ApJ, 549, L11
Miralda-Escudé, J., Cen, R., Ostriker, J. P., Rauch, M., 1996, ApJ, 471, 582
Muecket, J. P., Petitjean, P., Kates, R. E., & Riediger, R., 1996, A&A 308, 17
Netterfield, C. B., et al. 2001, ApJ, submitted (astro-ph 0104460)
Pryke, C., et al. 2001. ApJ, submitted (astro-ph 0104490)
Razoumov, A. O., Norman, M. L., Abel, T., & Scott, D. preprint (astro-ph 0109111)
Rauch, M., Miralda-Escudé, J., Sargent, W. L. W., Barlow, T. A., Weinberg, D. H., Hernquist, L., Katz, N., Cen, R., & Ostriker, J. P., 1997, ApJ 489, 7
Reisenegger, A. & Miralda-Escudé, J., 1995, ApJ 449, 476
Ricotti, M., Gnedin, N. Y., Shull, J. M., 2000, ApJ, 534, 41
Scherrer, R. J., & Weinberg, D. H., 1998, ApJ, 504, 67
Songaila, A., Hu, E. M., Cowie, L. L., & McMahon, R. G. 1999, ApJ, 525, L5
Schaye J., Theuns, T., Rauch, M., Efstathiou, G., Sargent, W. L. W., MNRAS, 318, 817
Schneider, D. P. et al. 2001, AJ, 121, 1232

Theuns, T., Leonard, A., Schaye, J., & Efstathiou, G. 1999, MNRAS, 303L, 58
Weinberg, D. H., Miralda-Escude, J., Hernquist, L., & Katz, N. 1997, ApJ, 490, 564
Zaldarriaga, M., Hui, L., & Tegmark, M., 2001, ApJ, 557, 519
Zhang, Y., Anninos, P., & Norman, M. L., 1995, ApJL, 453, L57
Zheng, W. et al. 2000, AJ, 120, 1607
Zuo, L. 1993, A & A, 278, 343
Zuo, L. & Phinney, E. S., 1993, ApJ, 418, 28

z	$\langle f \rangle$
4.5	0.25
5.2	0.09 ± 0.02
5.5	0.097 ± 0.002
5.7	0.070 ± 0.003
6.05	0.004 ± 0.003

Table 1: A summary of the observed mean transmission. The observation at redshift 4.5 is from Songaila et al. (1999). For this observation no error bars were provided by the authors. The observation at 5.2 is from Fan et al. (2000). The other observations are from Becker et al. (2001). Becker et al. (2001) have two observations at $z = 5.5$. The above mean transmission at $z = 5.5$ is the average of these two observations.

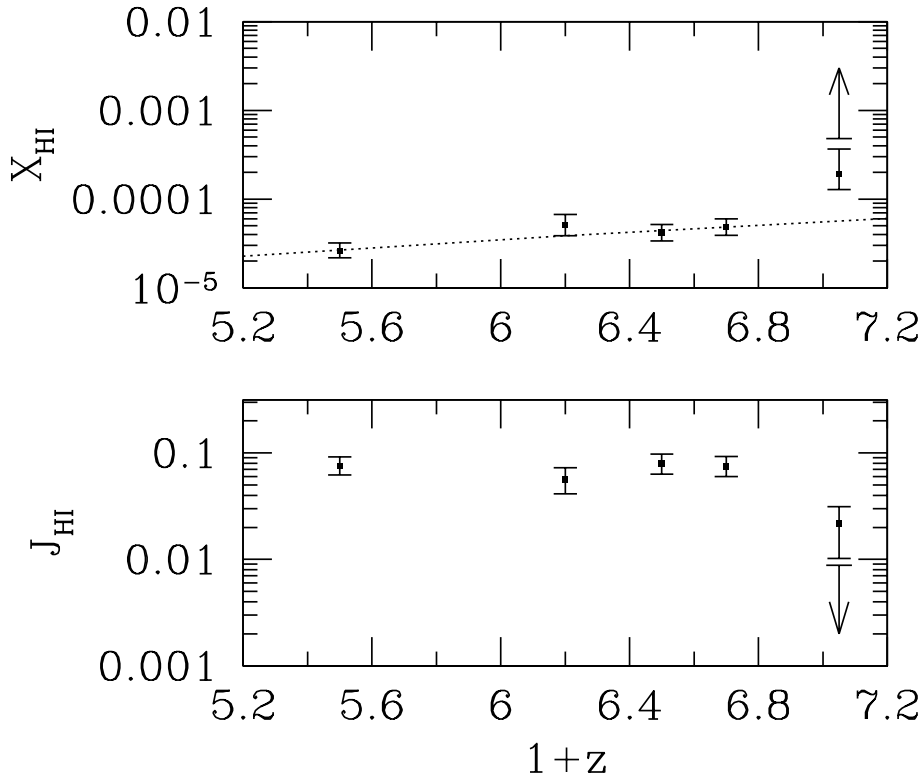

Fig. 1.— The top panel shows the neutral fraction of hydrogen at mean density as a function of redshift implied by the measurements of the mean transmission in the Lyα forest. The point with the error bar pointing towards a completely neutral IGM comes from matching the mean transmission in Lyβ. The error bars include the 1 σ uncertainty in power spectrum normalization and the 1 σ error in the observed mean transmission. The dotted line is offered as a guide to the eye. It shows $X_{\rm HI} = 3.5 \times 10^{-5}(1+z/6)^3$. The bottom panel shows the corresponding evolution in the ionizing background.

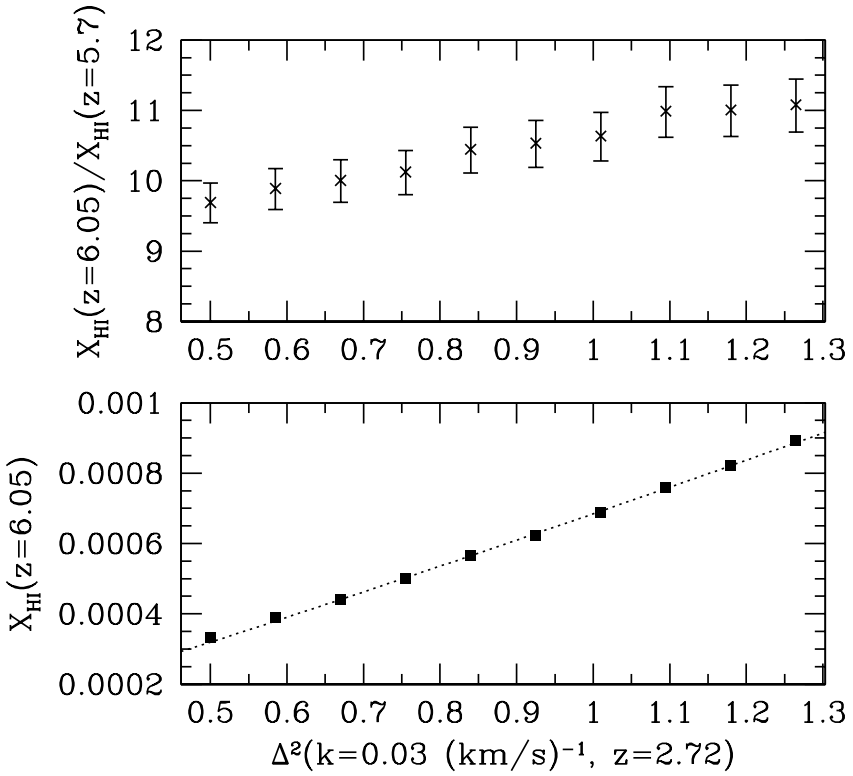

Fig. 2.— The upper panel shows the size of the jump in neutral fraction, $X_{\rm HI}(z = 6.05)/X_{\rm HI}(z = 5.7)$, as a function of power spectrum amplitude. The amplitude is described by the value of $\Delta^2(k) \equiv 4\pi k^3 P(k)/(2\pi)^3$ at $z = 2.72$ and velocity scale $k = 0.03(\,{\rm km/s})^{-1}$. $X_{\rm HI}(z = 6.05)$ corresponds to the lower limit arising from the 1 σ error in the mean transmission. The error bars come from the 1 σ uncertainty in the mean transmission at $z = 5.7$. The lower panel shows the neutral fraction itself at $z = 6.05$. The dotted line is $X_{\rm HI} = 5.8 \times 10^{-4}(\Delta^2(k)/0.86)^{1.1}$, demonstrating how the neutral fraction scales with amplitude.

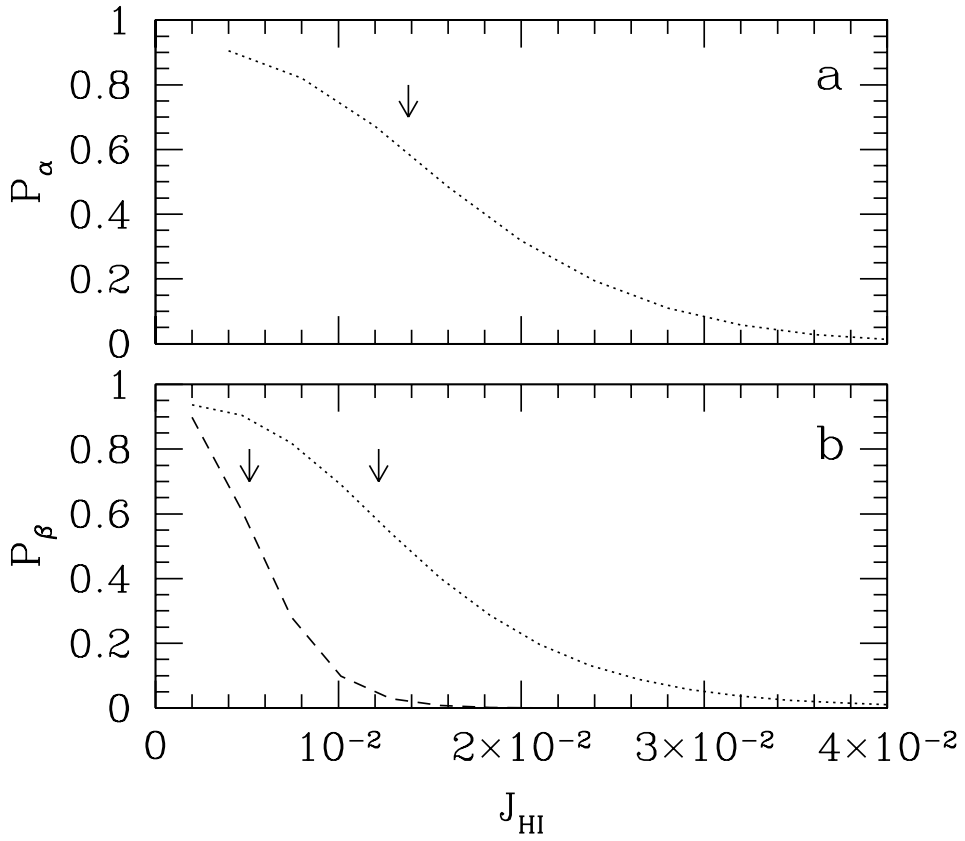

Fig. 3.— The upper panel a shows the probability $P_\alpha \equiv \int_{<F_m} P(F_1...F_N)dF_1...dF_N$ where F_i is the Lyα transmission at each pixel i of width $4\mathring{A}$. Here, $N = 60$, the noise per pixel is $\sqrt{\langle n^2\rangle} = 0.02$ and $F_m = 3\sqrt{\langle n^2\rangle}$. The lower panel b shows an analogous probability P_β except that F_i now contains both Lyα and Lyβ absorption. Here, $N = 48$, $\sqrt{\langle n^2\rangle} = 0.02$ and 0.005 for dotted and dashed line respectively. The arrows indicate the corresponding 1 σ upper limit on $J_{\rm HI}$ for these different probability distributions.

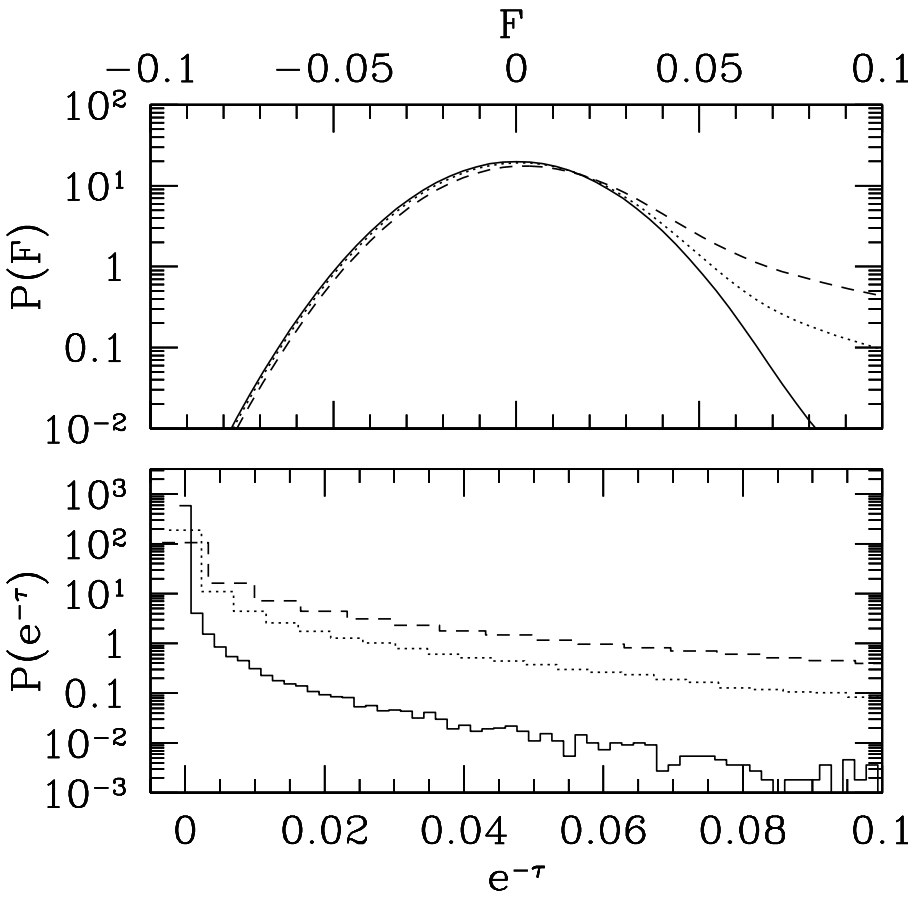

Fig. 4.— The lower panel shows the one-pixel ($4\mathring{A}$) probability distribution function of the true noiseless transmission $e^{-\tau}$ (i.e. $P(e^{-\tau})de^{-\tau}$ gives the probability) for 3 different values of $J_{\rm HI}$: 0.004 (solid), 0.012 (dotted) and 0.028 (dashed). The upper panel shows the probability distribution function of the noisy observed transmission F for the same three values of $J_{\rm HI}$. The negative values for F occur because of sky subtraction.

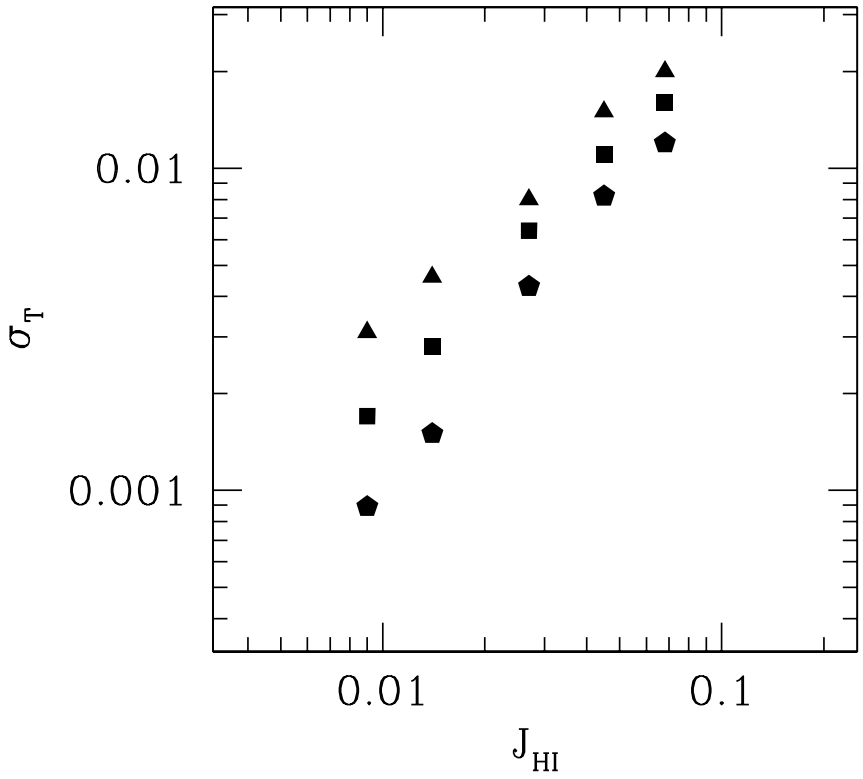

Fig. 5.— A prediction of the variance of the mean transmission, σ_T, (see Section 4) at $z \sim 6$, for several values of the ionizing background, $J_{\rm HI}$. The estimate ignores contributions from photon noise. The triangles are for a model with power spectrum normalization $\Delta^2(k = 0.03\,{\rm s/km}, z = 2.72) = 0.94$, the squares $\Delta^2(k = 0.03\,{\rm s/km}, z = 2.72) = 0.74$, and the pentagons $\Delta^2(k = 0.03\,{\rm s/km}, z = 2.72) = 0.58$.